A Compact QPSK Modulator with Low Amplitude and Phase Imbalance for Remote Sensing Applications

Farhan A. Ghaffar, Atif Shamim, M. Kashan Mobeen, Tareq Y. AlNafouri, Khaled N. Salama

Abstract: *A new, compact and wide-band Quadrature Phase Shift Keying (QPSK) modulator is presented for remote sensing applications. The microstrip-based modulator employs quadrature hybrid coupler, Wilkinson divider, rat race coupler and GaAs MESFET switches. It is designed to be part of an X band remote sensing transmitter with a center frequency of 8.25GHz. The fabricated module demonstrates the lowest reported amplitude and phase imbalances (0.1dB and 0.4° respectively) around its center frequency. The modulation, tested up to 160 Mbps data rate, displays carrier suppression greater than 30 dB. With negligible DC power consumption and low insertion loss, it operates for a wide bandwidth of 3 GHz (7-10 GHz). The effect of amplitude and phase imbalance is investigated on the performance of the modulator. Finally, a transmitter employing this modulator exhibits an excellent overall Error Vector Magnitude (EVM) of around 8 % that is considerably low as compared to the typically obtained values for such transmitters.*

Key Words: Quadrature Phase Shift Keying (QPSK) modulator, Error Vector Magnitude (EVM), Bit Error Rate (BER), Signal to Noise Ratio (SNR).

I. INTRODUCTION

Typically, transmitters designed for terrestrial and satellite applications were super heterodyne, employing modulation at some lower intermediate frequency (IF) and later on up converting to desired microwave or millimeter wave frequency [1]. However, in order to avoid complex and expensive architectures in super heterodyne transmission, modern systems have adopted direct carrier modulation or homodyne solution.

Mr. Farhan Abdul Ghaffar is a PhD student in Electrical Engineering Department, KAUST, Jeddah KSA (email: farhan.ghaffar@kaust.edu.sa), Dr. Atif Shamim (email: atif.shamim@kaust.edu.sa), Dr. Khaled Nabil Salama (email: khaled.salama@kaust.edu.sa) are Assistant Professors in Electrical Engineering Department, KAUST, Jeddah KSA., Dr. Tareq Al-Naffouri (email: tareq.alnaffouri@kaust.edu.sa) is an Associate Professor in Electrical Engineering Department, KFUPM, Dehran KSA, Mr. Kashan Mobeen (kashan..mobeen@gmail.com) is an alumnus of NED University of Engineering and Technology, Karachi, Pakistan.

Non-existence of the IF stage in a homodyne solution results in simple, compact and cost effective design for the microwave/millimeter wave regime. Several microwave digital communication links employ QPSK modulation as the preferred scheme for terrestrial [2] as well as satellite communications due to its ability to minimize Bit Error Rate (BER) [3-5]. In particular, QPSK modulation is employed to acquire data from wireless sensors in remote sensing applications.

A modulator plays a vital role in the transmit chain as its performance, in particular the amplitude and phase imbalance, is critical for the overall Signal to Noise Ratio (SNR), Error Vector Magnitude (EVM) and BER specifications of the complete transmitter. For remote sensing applications, the modulator must exhibit minimal amplitude and phase imbalance in order to minimize the EVM values of the transmitter. Various QPSK modulators have previously been reported in literature and performances of some of them have been summarized in Table 1. Some mixer-based designs have also been reported [1][2], however the large conversion loss and non-linearity are major issues for this approach. An alternate approach is the reflection type topology, which relies on switching action and partial reflection of signal for their operation. It can be observed from Table 1 that most of the modulators employ reflection type topology [3], [6-8] and demonstrate better performance in terms of phase and amplitude deviations in contrast to the mixer-based designs. The switching action can be done through schottky diodes [3], [9], HBTs [6] or MESFETs. However, the disadvantage of the Schottky diodes is high reverse leakage currents which cause thermal instabilities while the HBT's result in high amplitude and phase imbalance [6]. The issues mentioned above can be resolved using MESFETS as they provide high carrier mobility and excellent reverse recovery time which helps in overcoming high amplitude and phase deviations.

Our previous work [7], reported a reflection-type, microstrip based QPSK modulator. However, it was not a size efficient design (72 mm × 56 mm) as it employed multiple couplers and dividers. The new design reported in this paper employs only a single divider with a hybrid and a rat race coupler as compared to six elements in the previous design, thus reducing the overall size to one quarter (49 mm × 24 mm) of the modulator in [7]. Furthermore, it improves the phase imbalance and carrier

suppression and provides 1 GHz more bandwidth which is 12.12% better than the previous design. The design efficiently operates in the range of 7 GHz to 10 GHz with a data rate of up to 150 Mbps. This high data rate ensures the transmission of high-resolution images, which is a critical feature for remote sensing applications [5]. The new design exhibits amplitude imbalance of 0.1dB and phase imbalance of 0.3°, resulting in an EVM of 0.75% at a data rate of 160Mbps. The modulator for any data rate up to 160Mbps operates with an amplitude imbalance of less than 1% and phase imbalance of less than 0.4° resulting in an EVM of less than 1%. Finally, the modulator is integrated into an X band transmitter and the performance of the latter is investigated. Measurements reveal an EVM of 8% for a data rate of 160 Mbps. This value of EVM is in accordance with the international standard and considerably lowers than the typical values obtained from such transmitters [12].

The paper is distributed into five sections. Section II describes the theory and design of the modulator. Section III covers the implementation and operation, while Section IV explains the experimental results for both the standalone modulator and the transmitter employing this modulator and finally Section V analyses the performance of the modulator.

II. THEORY AND DESIGN

A. Theory

QPSK modulation is a type of Phase Shift Keying (PSK) in which carrier is modulated with two data bits from the data stream simultaneously. This results in one out of four possible carrier phase states i.e. 0°, 90°, 180° and 270°. For similar bandwidth, the information transfer rate of QPSK modulation is double than that of the Binary Phase Shift Keying (BPSK). Out of the two streams, one is In-phase (I) and the other is the Quadrature phase (Q), each with symbol rate equal to half that of the incoming bit rate. Both I and Q streams are mixed separately with two quadrature carriers resulting in two out-of-phase BPSK modulated signals 90°. QPSK signal is obtained by summing the two BPSK signals.

Mathematically, the four possible states can be expressed as:

$$S_{QPSK}=\sqrt{\frac{2Es}{Ts}}\text{Cos}\{(n-1)\frac{\pi}{2}\}\text{Cos}(2\pi f_c t) - \sqrt{\frac{2Es}{Ts}}\text{Sin}\{(n-1)\frac{\pi}{2}\}\text{Cos}(2\pi f_c t) \quad (1)$$

where n=1, 2, 3, 4

The above-mentioned four phases can be obtained using controlled microstrip phase shifting structures. This work employs couplers and MESFET switches to achieve the required phase shifting.

B. Design

The modulator is designed using three basic microwave couplers the Wilkinson divider, branch line hybrid coupler and the Rat Race Coupler. The three structures are designed utilizing AD 450 laminate of thickness 0.508 mm with a permittivity of 4.5. The width of a 50 Ω line, for these specifications of the substrate, is 0.94mm. The Wilkinson and hybrid couplers, used in this modulator, are designed with the help of bends instead of curves since the bends demonstrate better response at higher frequencies. Similarly for the sake of compactness, the rate race coupler is designed as a square ring rather than a circular one. In order to minimize the phase and amplitude imbalance, the s-parameters for the three elements are optimized at the carrier frequency. Figure 1 (a) shows the results with transmission coefficients to be around -3 dB and reflection coefficient to be less than -30 dB for all the three designs. Figure 1 (b) demonstrates that there is no phase shift between the two output ports of Wilkinson divider, 90° of phase shift between the two output ports of hybrid coupler and 180° of phase difference between the output ports of ring hybrid coupler. The results exhibit that the amplitude imbalance and phase imbalance of all the three elements are well within the acceptable range. The simulation results of these designs compare very well to the theoretical s-parameters of these microwave couplers. In order to minimize the phase/ amplitude imbalance and consequently the EVM of the modulator, the s-parameters of the couplers shall be optimized. All the simulations have been carried out in AWR's simulation tool, Microwave Office.

After the individual component design, the three microwave elements are integrated through MESFET switches to realize the complete modulator as shown in the schematic of Figure 2. The simulated power spectrum is shown in Figure 3 exhibiting a carrier suppression of greater than 30 dB which is expected from the design topology.

III. IMPLEMENTATION AND OPERATION

The layout implementation of the modulator is shown in Figure 4. The MESFETs are being driven by the data signals I, I', Q and Q'. The data bits drive the MESFET switches and make them toggle between on and off states. When the data bits are in high state the FET is in "ON" mode and allows the carrier to pass. On the contrary, when the data bits are in the low state, the MESFET is in "OFF" mode and the carrier is reflected back. That is why this modulators topology is known as the reflection type. The data signals force the MESFETs into their ON and OFF states. Carrier of frequency 8.25GHz is launched from the input port (port 1) of Wilkinson divider which provides an equal split of the signal. The output ports (ports 2 and 3) of the Wilkinson are connected to the two MESFET (model CFY25) switches operated by the data streams Q and Q′.

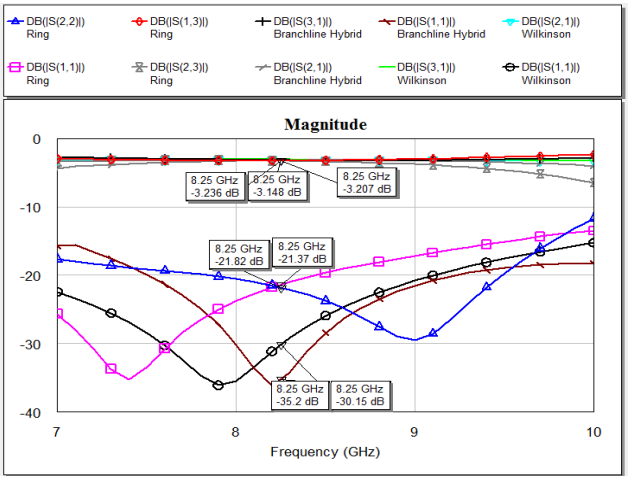

Fig. 1(a) Amplitude response of the three couplers

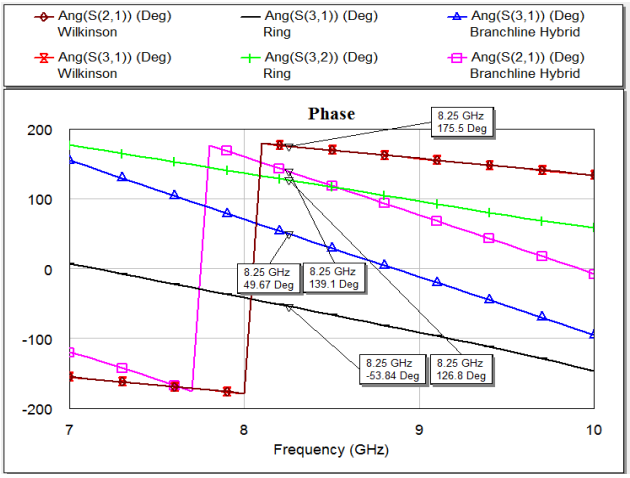

Fig. 1(b): Phase response of the three couplers

TABLE I

COMPARISON OF THE MODULATOR WITH THE PREVIOUSLY PUBLISHED WORK

Ref	Tech.	Freq. (GHz)	Phase Dev. (Degree)	Amplitude Dev. (dB)	Carrier Supp. (dB)	Bandwidth (GHz)	Insertion Loss (dB)	Comments
[1]	PCB	8.3	10	2	>25	-	13	Large phase and amplitude imbalance and high insertion loss
[2]	PCB	21-24	7	0.5	22	3	8	Impractical phase imbalance
[3]	IC	2.75-4.75	5	0.5	27	2	9-10	Large phase and amplitude imbalance
[4]	IC	7.2-8.5	5	1	>30	1.3	-	Phase imbalance and amplitude imbalance are too high.
[6]	PCB	24-32	2	0.4	-	8	11-19	High Insertion loss and phase imbalance
[7]	PCB	8.25	<0.5	0.1	29	2	<10	Large size and small bandwidth
[8]	PCB	1.5	<2	0.5	-	0.5	8	Large EVM (5%)
[9]	PCB	27	<2	-	25	1	6.7	Phase Imbalance is large
[10]	PCB	28.4	5	0.5	-	-	6.5	Large phase and amplitude imbalance
[11]	IC	60	3	0.5	>20	4	13.5	High Insertion loss and phase imbalance
This Work	PCB	8.25	<0.4	0.1	>30	3	<9.5	Small imbalances resulting in EVM of less than 1%

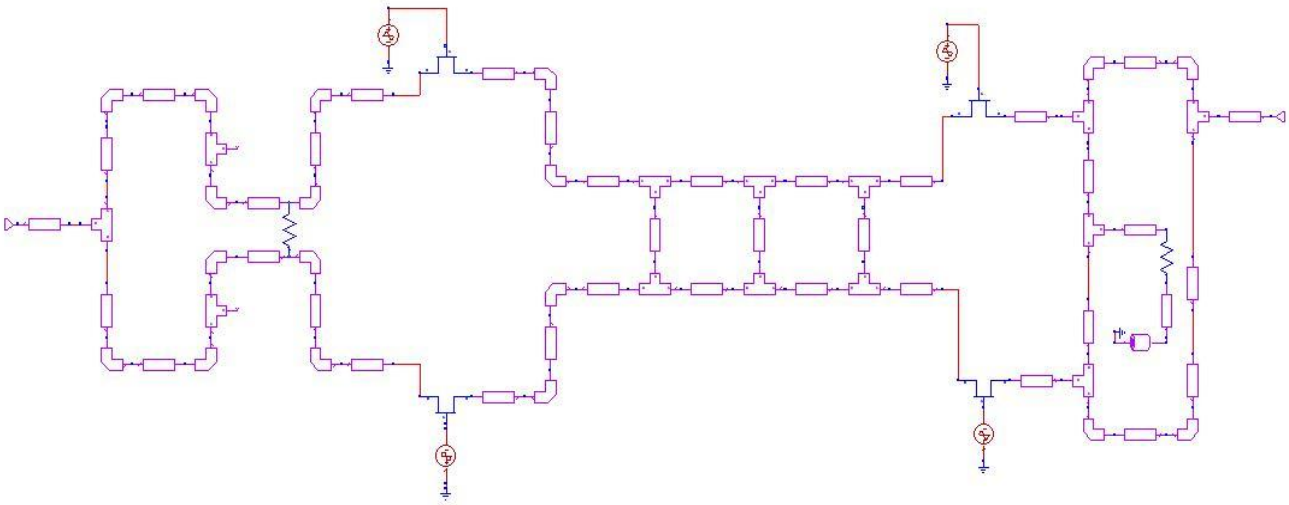

Fig. 2: Schematic of the Modulator

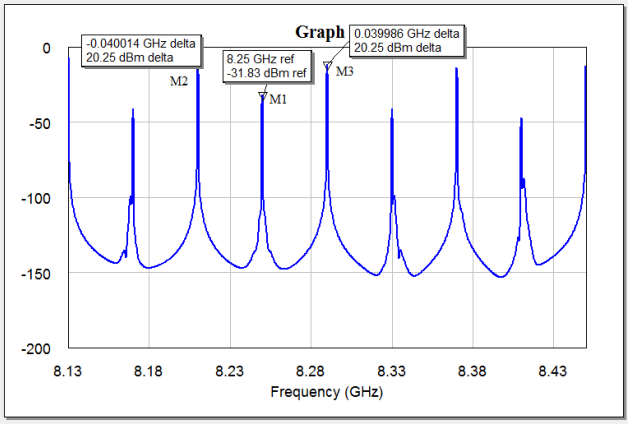

Fig. 3: System Simulation of the Modulator

The nature of the bit streams suggest that there will be only one of the switches that will allow the carrier to flow through it for instance if Q is at logic 1 than Q′ will be at logic 0 and vice versa. Both the signals have a zero phase shift between them. The signal allowed to go through will be launched at one of the two input ports (ports 1 or 4) of branchline hybrid coupler. This coupler will further divide the carrier signal into two parts of equal magnitude but 90° apart from each other. The two output ports (ports 2 and 3) of the hybrid coupler are connected to the two MESFET switches operated by data streams I and I′.

Like before, signal from one of the ports passes through the MESFET which is on and is incident on one of the input ports (ports 1 and 2) of the rat race coupler. This coupler either passes the carrier without any phase shift or with a phase shift of 180°, depending upon which input has been used.

The phase shift that will be produced by different data symbols is shown in Figure 5. As it can be seen that for symbol ‘00’ there is no phase shift in either of the couplers hence producing 0° phase shift at the output of the modular. However for the data symbol ‘10’ hybrid coupler will produce a phase shift of 90° where as rat race coupler does not produce any phase shift in the signal resulting in a total phase shift of 90°. In the same way the other two data symbols i.e. ‘11’ and ‘01’ will produce phase shifts of 180° and 270° respectively. In the above figure Wilkinson has not been considered because the relative phase shift at the output of Wilkinson is 0°.

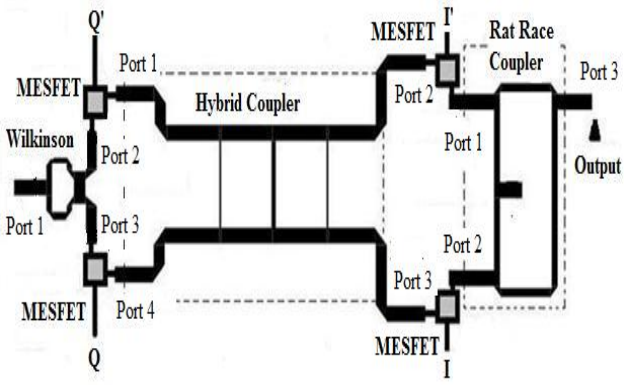

Fig. 4: Modulator Implementation

IV. FABRICATION AND MEASUREMENT

The design is fabricated on a 0.508 mm thick Arlon’s Printed Circuit Board (PCB) through a chemical etching process. The MESFET switches are soldered on the PCB, which is then mounted on Aluminum housing as shown in Figure 6. Aluminum housing is required due to the fact that AD450 has very small thickness and SMA connectors cannot be mounted on it directly therefore a housing is used on which SMA connectors can be easily mounted and this will make the testing of the modulator very convenient. SMA connectors with extended Teflon are used which are

mounted on the housing. The Teflon's length was kept exactly equal to the width of the housing's wall. The launching pin of the SMA was kept exactly at the center of the feed line both at the input and output. This ensures for the minimum mismatch between the SMA and the feed line.

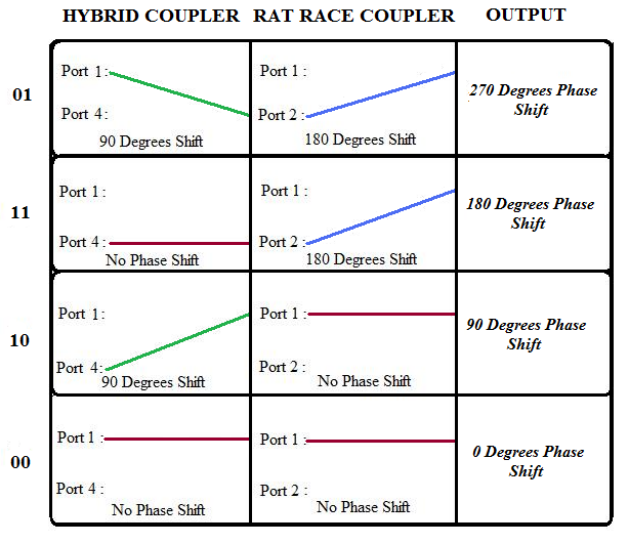

Fig. 5: Signal flow diagram of modulator for different data symbols

The test setup comprise a signal generator providing the carrier frequency of 8.25 GHz, two data sources which will generate I and Q data sequences along with their complements I´ and Q´, and a signal analyzer to observe the spectrum and constellation diagram of the modulator. The insertion loss is measured using a network analyzer with modulator being in static state (static state means that the modulator is provided with one symbol of data). The Modulator is tested up to a data rate of 160 Mbps (80 Mbps each on I and Q channel). The spectrum obtained exhibits a carrier suppression of greater than 32 dB with a phase imbalance of less than 0.4° and an amplitude imbalance of less than 1% (0.1dB). Table 2 summarizes the results of QPSK modulator at different frequencies. As expected, the amplitude and phase imbalance obtained at the centre frequency (8.25 GHz) are minimum, while at other frequencies the phase and amplitude deviations increase. Table 3 demonstrates the results for varying data rates. It can be observed that with increasing data rate, the amplitude and phase deviations increase. The measurement setup allowed a maximum data rate of 160 Mbps for which the amplitude and phase deviations remained under acceptable range.

The insertion loss of the modulator is measured to be less than 9.5 dB for a carrier frequency of 7 GHz to 10 GHz. This insertion loss is acceptable for the entire range of frequency. Similarly the carrier suppression of greater than 30 dB is achieved for a bandwidth of 3GHz. The measured insertion loss and carrier suppression versus the carrier frequency are shown in Figures 7 and 8 respectively. The measurement result show that the insertion loss of the modulator increases with the increase in the applied data rate, which is expected. The insertion loss is 9.48 dB for a baseband bandwidth of 80MHz. It can be deduced from Figure 9 that insertion loss of the modulator never exceeds 9.5 dB.

Figure 10 shows the constellation diagram obtained while testing the modulator at 8.25 GHz carrier frequency and a data rate of 160 Mbps. A phase imbalance of 0.3° and magnitude imbalance of 0.1dB (0.54%) is observed which is very close to 0dB of simulated result. It can also be observed on the right side of the figure that the analyzer recovers the data stream that has been modulated. The spectrum obtained under the same conditions is shown in Figure 11. It demonstrates a carrier suppression of more than 30 dB, and the side lobe suppression of greater than 40dB for an input power of 0 dBm. The resolution bandwidth of spectrum analyzer was set to 3MHz while the video bandwidth was set to 10MHz.

The modulator is tested for a carrier input power of 0 dBm. In the transmitter the power at the output of the up converter is 0 dBm. The modulator is connected to the output of the up converter in the transmitter chain and therefore the modulator will receive an input RF power of 0 dBm. Keeping this in view all the measurements are done for an RF power of 0dBm.

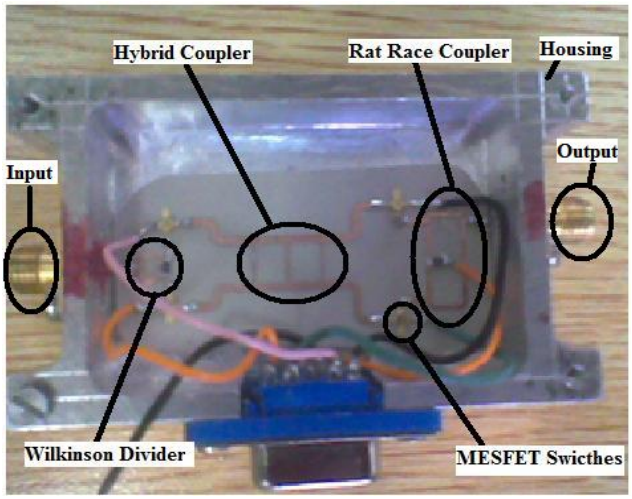

Fig. 6: Fabricated Modulator on Arlon's AD 450 PCB

V. PERFORMANCE ANALYSIS

Phase and amplitude imbalance are the important parameters, which affect the BER of the modulator. The two together determine the Error Vector Magnitude (EVM). EVM is the

measurement or vector, taken in terms of peak or rms percentages, between the ideal symbol position and the actual measured position on the constellation diagram. The concept is shown in Figure 12, where the magnitude of the vector drawn from (I_o, Q_o) to (I_s, Q_s) represents EVM. I_o and Q_o represent the ideal symbol position, while I_s and Q_s represent the actual measured symbol position on the constellation diagram.

The designed modulator demonstrates excellent EVM values at different data rates, as shown in Table 4. For the highest data rate of 160 Mbps, the EVM value is less than 0.8%. As expected, the value of EVM increases as the data rate increases.

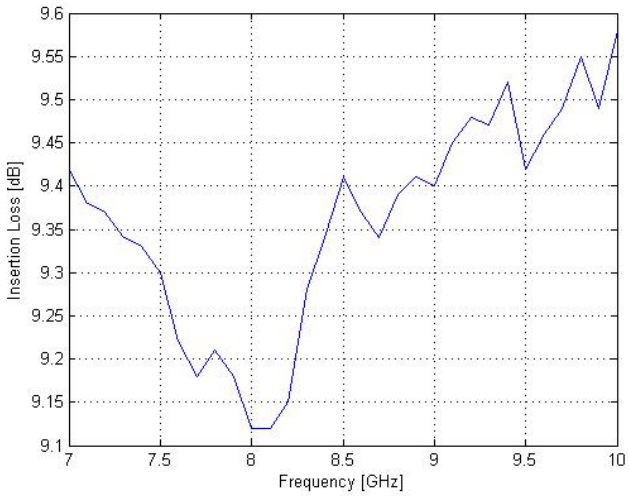

Fig. 7: Insertion Loss vs. Carrier Frequency

TABLE II

MEASURED RESULTS AT DIFFERENT CARRIER FREQUENCIES

Frequency (GHz)	Amplitude Imbalance (dB)	Phase Imbalance (deg)	Carrier Suppression (dB)
7.9	0.12	0.36	30.3
8.25	0.1	0.30	32.3
8.4	0.142	0.38	29.8

EVM is the figure of merit for a modulator. EVM can be related to the SNR through (2).

$$\text{EVM} \propto \frac{1}{\sqrt{SNR}} \qquad (2)$$

Probability of error (P_e) for a QPSK modulator is given as,

$$P_e = 2Q\left(\sqrt{2SNR}\right)\text{-}Q^2\left(\sqrt{2SNR}\right) \qquad (3)$$

The Q function used in equation (3) is defined as the tail probability of the standard normal distribution. Q(x) is the probability that a normal standard random variable will obtain a value larger than value of x.

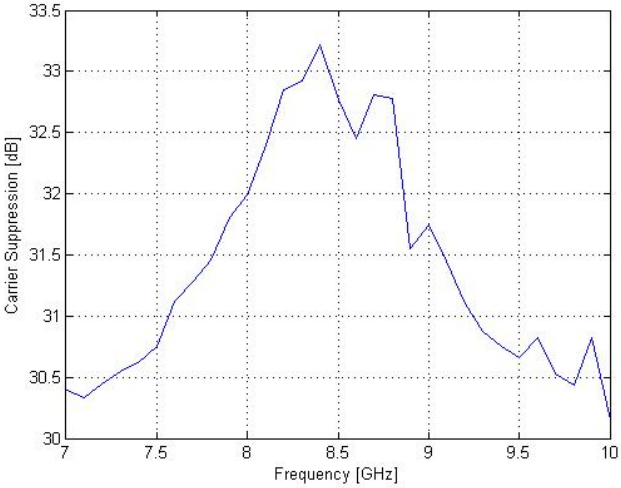

Fig. 8: Carrier Suppression vs. Carrier frequency

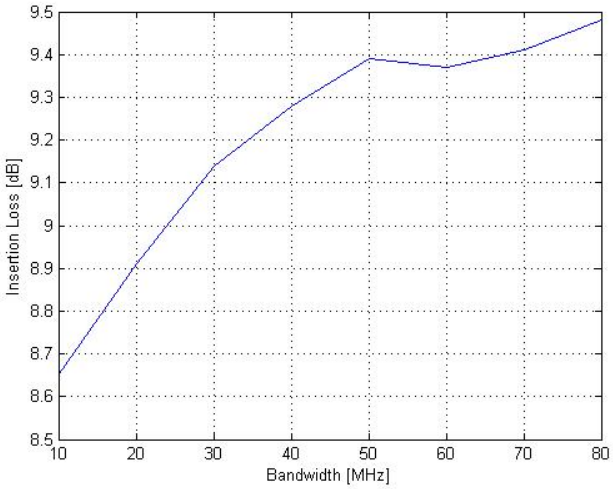

Fig. 9: Insertion Loss vs. Baseband Bandwidth

TABLE III

MEASURED RESULTS AT DIFFERENT DATA RATES

Data Rate (Mbps)	Amplitude Imbalance (dB)	Phase Imbalance (deg)	Carrier Suppression (dB)
160	0.1	0.30	32.3
120	0.09	0.25	34.4
80	0.075	0.15	37.1

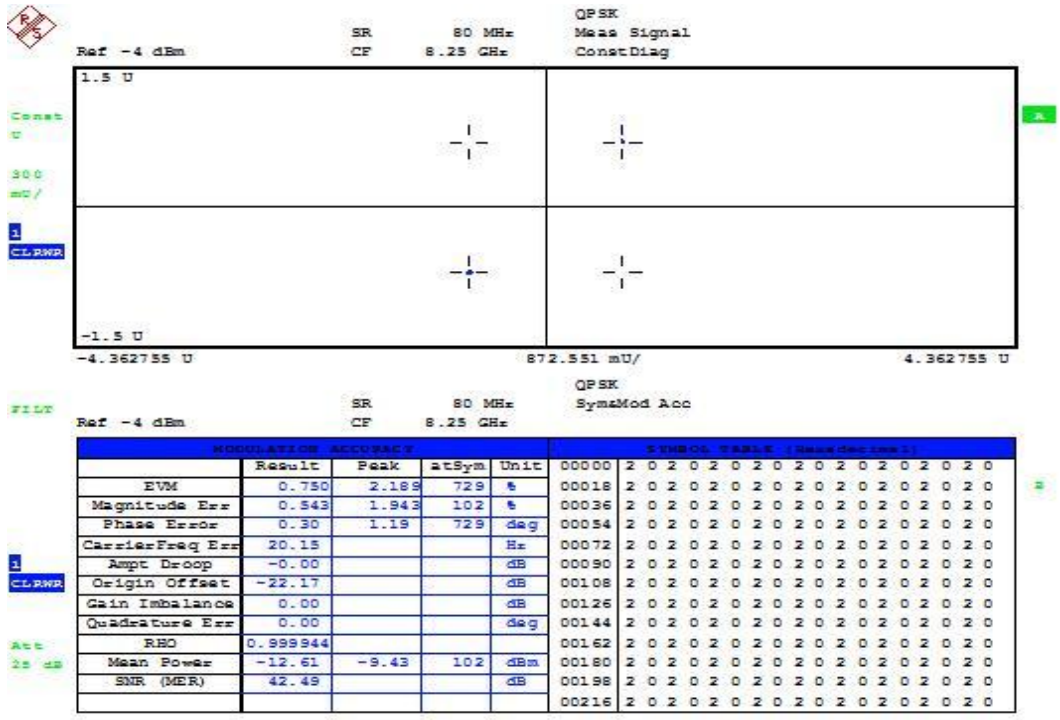

Fig. 10: Constellation Diagram of the Modulator

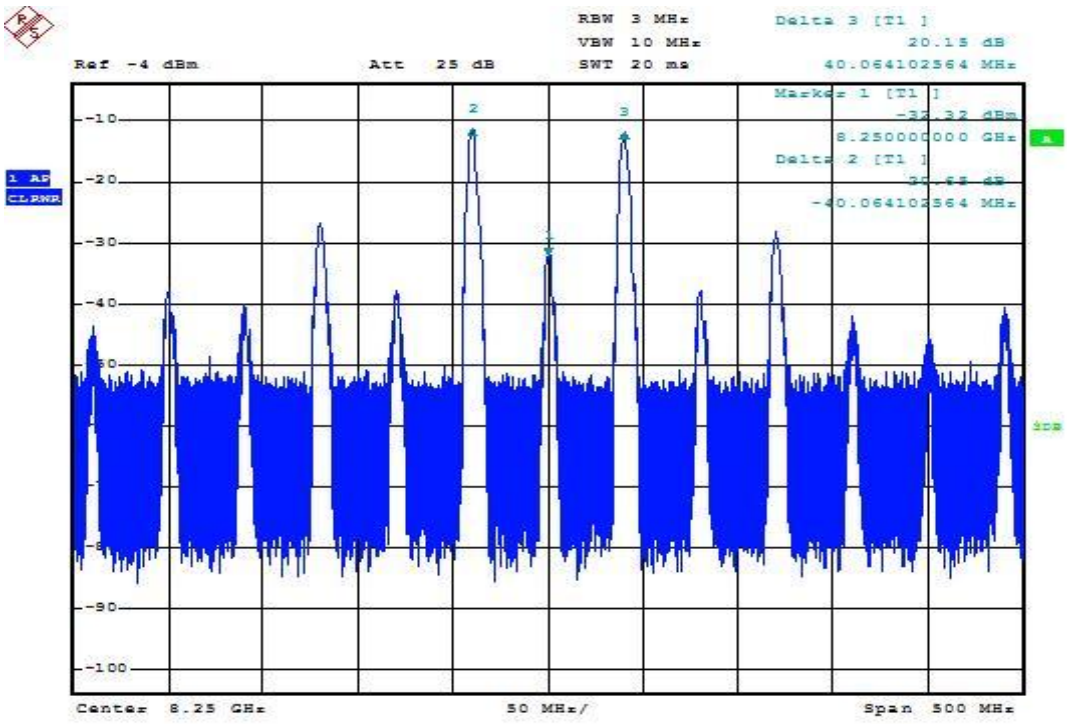

Fig. 11: Measured Spectrum of the Modulator

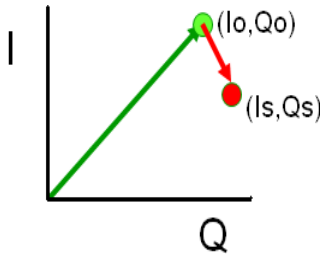

Fig. 12: EVM description

TABLE IV

MEASURED EVM VALUES AT DIFFERENT DATA RATES

Data Rates (Mbps)	EVM (%)
160	0.750
120	0.479
80	0.368

The probability of error depends on the SNR according to equation (3) which indirectly relates it to EVM as SNR is related to EVM. It is clear from (2) and (3) that in order to minimize probability of error, the value of SNR must be maximized, which in turn requires a smaller EVM value. Since EVM is dependent on amplitude and phase imbalance, a modulator optimized for small amplitude and phase deviation results in lower EVM, higher SNR and eventually low P_e. Such modulator performance is important for the overall transmitter performance, as will be shown in the next section.

A. Integration of the Modulator in Transmitter

In order to assess the performance of the modulator at the system level, it is integrated in an X-band transmitter, as shown in the block diagram of Figure 13. The transmitter chain consists of a Local Oscillator (LO) that provides the carrier frequency of 8.25GHz with phase noise of -100dBc/Hz at 10kHz and output power of 0dBm, a band pass filter for out of band signal rejection, with a 3 dB bandwidth of 100MHz and centre frequency of 8.25GHz, a power amplifier to boost the RF power with a gain of 4dB and 1dB compression point of 37dBm. Finally a low pass filter to reject the higher order harmonics of the carrier frequency at cut off frequency of 8.5 GHz with insertion loss of 1dB. After integration in the transmitter, the modulator is tested at a data rate of 160 Mbps through data sources and a vector signal analyzer. The results are summarized in Table 5.

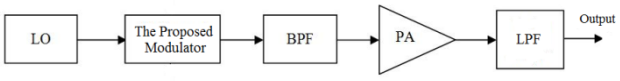

Fig. 13: Integration of Modulator in a Transmitter

TABLE V

RESULTS OF MODULATOR AFTER INTEGRATION IN TRANSMITTER

Frequency (GHz)	Data Rate (Mbps)	EVM (%)	Phase Imbalance (Degree)	Amplitude Imbalance (%)
8.25	160	7.67	1.5	6.78 (1.4dB)

EVM of the entire transmitter is found to be less than 8% which is in accordance with the IEEE *802.11aTM-1999* standard [13] compares the BER and EVM of a QPSK modulated transmitter. The reason for the degradation of the EVM of the transmitter is the presence of the power amplifier in the transmitter chain. This is verified by two separate sets of EVM measurements, done with and without the power amplifier in the transmit chain (See Fig. 13). The measurement without the power amplifier shows that the EVM degradation is negligible after the filter stage. However, the measurement with the power amplifier shows that the major EVM degradation happens after the power amplifier. It is observed that as long as EVM of the transmitter is below 20%, the BER value remains less than 10^{-6}. A BER of 10^{-6} is quite suitable for remote sensing applications. The EVM of design under discussion is even lower (8%), so the expected BER will be of the order of 10^{-12}.

VI. CONCLUSION

The paper presents a novel design for a compact and wide-band QPSK modulator based on reflection type topology. The modulator, fabricated in the standard PCB technology, exhibits one of the lowest reported values for amplitude and phase imbalance (0.1 dB and 0.4° respectively) at the center frequency of 8.25 GHz. The modulation tested up to a data rate of 160 Mbps displays carrier suppression greater than 30 dB and an EVM of 0.8%. With low DC power consumption and insertion loss, it operates for a wide bandwidth of 3 GHz (7-10 GHz). Measurements on an X-band transmitter employing this modulator reveal an EVM of around 8 % that is considerably lower as compared to the typically obtained values for such transmitters.

REFERENCES

[1] M. Siddiqua**, "**Design and Analysis of X Band QPSK Modulator using Direct Carrier Technique," *Multitopic Conference, 2006, INMIC'06, p.106-110.*

[2] B. Jokanovic, S. Stojanovic and M.Peric, "Direct QPSK Modulator for Point-to-Point Radio link at 23GHz," *5th Conference on Telecommunication in Modern Satellite, Cable and Broadcasting Service,*

2001. TELSIKS 2001, vol.1, p. 217-220.

[3] S. Kumar and G. Wells, "2.75-4.75GHz QPSK Modulator with low amplitude and phase errors," *Electronic letters, vol. 26, no. 14, 1990, pp.961-962*.

[4] N. Cartier, N. Hussonnois, B. Traneir, P. Maynadier, E. Midan, M. Sutter, P. Boutet, H. Buret and A. Clerino, " X Band Full MMIC QPSK Modulator with Direct Oscillator for Spot 5 Earth Observation Satellite Payload," *29th European Microwave Conference,1999, vol.1, p.115-118.*

[5] O. Belce, "Comparison of Advanced Modulation Schemes for LEO Satellite Downlink Communications," *International Conference on Proceedings of Recent Advancement in Space Technologies, 2003, RAST'03, p. 432-437.*

[6] Yi Sun, A.P. Freundorfer and D. Swatzky, "A QPSK Direct Digital Modulator in GaAs HBT at 28GHz," *Canadian Conference on Electrical and Computer Engineering, 2005, p. 1882-1885.*

[7] F.A. Ghaffar, M.K. Mobeen, S. Qamar and M. Hasan, "A Wide-Band QPSK modulator using Branch Line Coupler and MESFET Switches," *52nd IEEE Midwest Symposium on Circuits and Systems, 2009, MWSCAS'09, p.1014-1017.*

[8] T. Pochirju and V.F. Fusco, "Ultra-Low Power High Bandwidth QPSK Modulator," *International microwave Symposium Digest, 2008, IEEE MTT-S, p. 9-12.*

[9] H. Ogawa and M. Akaike, "Integrated Balanced BPSK and QPSK Modulators for the Ka-Band," *IEEE Transactions on Microwave Theory and Techniques, 1982, vol.30, no. 3, pp. 227-234.*

[10] G.B. Gajda and C.J. Verver, "Millimeter wave QPSK Modulator in Fin line," *International Microwave Symposium Digest, IEEE MTT-S, 1987, vol.86, no.1, p. 233-236.*

[11] A. Grotte and Kai Chang, "60GHz Integrated- Circuit High Data Rate Quadriphase Shift Keying Exciter and Modulator," *IEEE Transactions on Microwave Theory and Techniques, 1984, vol.32, no.12, pp. 1663-1667.*

[12] Applied Wave Research Microwave Office™ "http://web.awrcorp.com/Usa/Products/Microwave-Office."

[13] Maoliu Lin, Qijun Zhang and Qinghua Xu, "EVM Simulations and its Comparison with BER for Different Types of Modulations," *IEEE Region 10 Conference, 2007, TENCON, 2007, p. 1-4.*

[14] G. Flower, R. Dugan, J. Zhang, J. Chang and P.Petruno, "QPSK Modulator for Digital Cellular Communication," *Proceedings of the 1992 Bipolar/BiCMOS Circuits and Technology Meeting, 1992, p. 59-62.*

[15] R.S. Bokulic "Design of Differential QPSK Modulator," *Electronic Letters, vol. 27, no.13, 1991, pp. 1185-1186.*

[16] John G. Proakis "Digital Communication," 4th Edition, McGraw-Hill, 2000.

BIOGRAPHIES

Farhan A. Ghaffar received his B.E. degree in electronics engineering from Nadirshaw Eidulji Dinshaw (NED) University of Science and Technology, Karachi, Pakistan in 2007 and the M.S degree in electrical engineering from King Abdullah University of Science and Technology (KAUST), Thuwal, Saudi Arabia in 2010. He is currently a PhD student in electrical engineering program of King Abdullah University of Science and Technology.

Before joining KAUST Mr. Ghaffar was an Assistant Manager at Pakistan Space and Upper Atmosphere Research Commission (SUPARCO) from January 2008 to August 2009. His research interests involve design of System on Package (SoP) and System on Chip (SoC) based antennas, radio frequency integrated circuits (RFICs) and ferrite Low Temperature Co-fired Ceramic (LTCC) based tunable antennas and passives.

Atif Shamim (S'03-M'09) received his M.A.Sc. and Ph.D degrees in electrical engineering at Carleton University, Canada in 2004 and 2009 respectively. He was an NSERC Alexander Graham Bell Graduate scholar at Carleton University from 2007 till 2009 and an NSERC postdoctoral Fellow from 2009-2010 at King Abdullah University of Science and Technology (KAUST), KSA. In August 2010, he joined the Electrical Engineering Program at KAUST, where he is currently an Assistant Professor. He was an invited researcher at the VTT Micro-modules Research Center (Oulu, Finland) in 2006.

Dr. Shamim was the recipient of the best paper prize at the EuWiT Conference in the EuMA week (2008). He was given the Ottawa Centre of Research Innovation (OCRI) Researcher of the Year Award (2008). His work on "Wireless Dosimeter" won the ITAC SMC Award at Canadian Microelectronics Corporation TEXPO (2007). He received the best student paper finalist prize at IEEE APS conference in 2005. His research interests are in integrated on-chip antennas, low power CMOS RFIC's for system-on-chip (SoC) applications and advanced system-on-package (SoP) designs employing multilayer LTCC and LCP packaging technologies.

M. Kashan Mobeen received his B.E. degree in Electronic Engineering from NED University of Engineering and Technology, Karachi, Pakistan. He is currently perusing M.S. in the feild of Electronic Engineering. He has published two papers in national and international conference preceedings. His research interests includes microwave communications and RF transmission systems especially modulation techniques.

Tareq Y. AlNafouri (S'03-M'09) received his B.S. degrees in mathematics and electrical engineering (with First Honours) from King Fahd University of Petroleum and Minerals, Dhahran, Saudi Arabia in 1994, the M.S. degree in electrical engineering from Georgia Institute of Technology, Atlanta, in 1998 and the PhD degree in electrical engineering from Stanford University, CA, in 2004.

He was a visiting scholar at the California Institute of Technology, Pasadena, from January to August 2005 and during summer 2006. He was a Fulbright scholar at the University of Southern California from February to September 2008. He has held internship positions at NEC Research Labs, Tokyo, Japan in 1998; the Adaptive Systems Lab, University of California at Los Angeles in 1999; National Semiconductor, Santa Clara, CA, in 2001 and 2002; and Beceem Communications, Santa Clara, CA, in 2004.

He is currently an Associate Professor at the Electrical Engineering Department, King Fahd University of Petroleum and Minerals, Saudi Arabia. Since November 2008, he has been serving as the Director of the Office of Cooperation with King Abdullah University of Science & Technology (KAUST). His research interests lie in the areas of adaptive and statistical signal processing and their applications to wireless communications, seismic signal processing, and in multiuser information theory. He has recently been interested in compressive sensing and random matrix theory and their applications. He has over 60 publications in journal and conference proceedings, nine standard contributions, and one issued patent and four pending patents.

Dr. Al-Naffouri is the recipient of a 2001 Best Student Paper Award at the I EEE-EURASIP Workshop on Nonlinear Signal and Image Processing (NSIP) 2001 for his work on adaptive filtering analysis, the IEEE Education Society Chapter Achievement Award in 2008, and Al-Marai Award for innovative res earch in communication in 2009.

Khaled N. Salama received the Bachelor's degree (with honors) from Cairo University, Giza, Egypt, in 1997 and the Master's and Doctoral degrees from Stanford University, Stanford, CA, in 2000 and 2005, respectively.

Between 2005 and 2008, he was an Assistant Professor with the Department of Electrical, Computers and Systems Engineering, Rensselaer Polytechnic Institute, Troy, NY. He cofounded Ultrawave labs, a medical imaging startup, in 2007, and serves as its Vice President of Research and Development. Since Fall of 2009, he has been an Assistant Professor of electrical engineering and its founding acting program chair with the King Abdullah University of Science and Technology, Thuwal, Saudi Arabia. He has coauthored 50 papers and four patents in the areas of biosensors, low-power mixed-signal circuits for intelligent sensors, and medical instrumentation.

Dr. Salama was elected to the IEEE Sensory Systems and the IEEE Bio- Circuits Technical Committees in 2006 and to the IEEE VLSI Systems and Applications Committee in 2007. He is currently the Tutorial Chair of the IEEE BioCircuits Conference and the Association for Computing Machinery Great Lakes VLSI Symposium. His work on low-light detection and fully integrated imagers has been funded by the U.S. Defense Advanced Research Projects Agency and the National Institutes of Health, was awarded the Stanford–Berkeley Innovators Challenge Award in biological sciences, and was recently acquired by Lumina Inc.